EMBO reports

scientific report

Vesicular stomatitis virus inhibits mitotic progression and triggers cell death

Papia Chakraborty[1], Joachim Seemann[1], Ram K. Mishra[2], Jen-Hsuan Wei[1], Lauren Weil[1], Daniel R. Nussenzveig[3,4], Joshua Heiber[5], Glen N. Barber[5], Mary Dasso[2] & Beatriz M.A. Fontoura[1+]

[1]Department of Cell Biology, University of Texas Southwestern Medical Center, Dallas, Texas, USA, [2]Laboratory of Gene Regulation and Development, National Institute of Child Health and Human Development, National Institutes of Health, Bethesda, Maryland, USA, [3]Department of Pathology, University of Texas Southwestern Medical Center, [4]Pathology and Laboratory Medicine Service, Veterans Affairs North Texas Health Care System, Dallas, Texas, USA, and [5]Department of Medicine and Sylvester Cancer Center, University of Miami School of Medicine, Miami, Florida, USA

Vesicular stomatitis virus (VSV) infects and kills a wide range of cell types; however, the mechanisms involved in VSV-mediated cell death are not fully understood. Here we show that VSV infection interferes with mitotic progression, resulting in cell death. This effect requires the interaction of VSV matrix (M) protein with the Rae1–Nup98 complex in mitosis, which is associated with a subset of ribonucleoproteins (RNPs). VSV displaced Rae1 from spindle poles, caused spindle abnormalities and triggered substantial cell death during metaphase. These effects were attenuated in cells infected with VSV expressing a mutant M protein that does not bind efficiently to the Rae1–Nup98–RNP complex. In cells that progressed to late mitosis, M protein prevented proper nuclear formation and chromatin decondensation. VSV is an oncolytic (anti-tumour) agent as it preferentially replicates and kills tumour cells. As tumour cells have a high mitotic index, VSV-mediated mitotic cell death probably contributes to its oncolytic activity.

Keywords: nuclear pore complex; nucleoporins; mRNA export; mitosis; spindle assembly

EMBO reports (2009) **10**, 1154–1160. doi:10.1038/embor.2009.179

INTRODUCTION

Vesicular stomatitis virus (VSV) is an enveloped virus with a negative strand RNA genome, which encodes five proteins. One of the crucial functions of VSV matrix (M) protein in the host cell is to prevent antiviral gene expression. M protein inhibits nuclear export of messenger RNAs (Her *et al*, 1997; von Kobbe *et al*, 2000; Enninga *et al*, 2002; Faria *et al*, 2005) by interacting with constituents of the mRNA export machinery, the mRNA export factor Rae1 and the nucleoporin Nup98 (von Kobbe *et al*, 2000; Faria *et al*, 2005). These interactions result in bulk mRNA export block from the nucleus, and consequently, inhibition of gene expression (Her *et al*, 1997; von Kobbe *et al*, 2000; Enninga *et al*, 2002; Faria *et al*, 2005). During mitosis, the Rae1–Nup98 complex acquires further functions essential for spindle assembly (Blower *et al*, 2005; Wong *et al*, 2006) and maintenance of the mitotic checkpoint (Jeganathan *et al*, 2005).

VSV is one of the RNA and DNA viruses that have shown significant anti-tumour (oncolytic) efficacy—that is, they replicate and preferentially kill cancer cells as compared with normal cells (Stojdl *et al*, 2003; Balachandran & Barber, 2004; Barber, 2005). This oncolytic activity is due, at least in part, to impaired interferon responses in tumour cells during interphase, but further unknown factors and/or pathways are probably involved (Barber, 2005). Owing to its oncolytic characteristic, VSV is now being considered for cancer therapy. We show here that during VSV infection or in the presence of M protein alone, cells can undergo death during mitosis after inhibiting spindle assembly and nuclear formation, which involves disruption of Rae1 functions. Thus, these mitotic defects mediated by VSV will probably trigger the death of tumour cells, which have a high mitotic index.

RESULTS AND DISCUSSION

VSV induces cell death during mitosis through M protein

As VSV M protein interacts with the Rae1–Nup98 complex during interphase (von Kobbe *et al*, 2000; Faria *et al*, 2005) and this complex has additional functions during mitosis (Blower *et al*, 2005; Jeganathan *et al*, 2005; Wong *et al*, 2006), we investigated whether VSV infection interferes with mitotic progression. We also analysed VSV interference with G1 progression for comparison.

[1]Department of Cell Biology, University of Texas Southwestern Medical Center, 5323 Harry Hines Boulevard, Dallas, Texas 75390, USA
[2]Laboratory of Gene Regulation and Development, National Institute of Child Health and Human Development, National Institutes of Health, Bethesda, Maryland 20892, USA
[3]Department of Pathology, University of Texas Southwestern Medical Center, Dallas, Texas 75390, USA
[4]Pathology and Laboratory Medicine Service, Veterans Affairs North Texas Health Care System, Dallas, Texas 75216, USA
[5]Department of Medicine and Sylvester Cancer Center, University of Miami School of Medicine, Miami, Florida 33136, USA
[+]Corresponding author. Tel: +1 214 648 9535; Fax: +1 214 648 8694;
E-mail: beatriz.fontoura@utsouthwestern.edu

Received 16 January 2009; revised 21 June 2009; accepted 23 June 2009; published online 11 September 2009

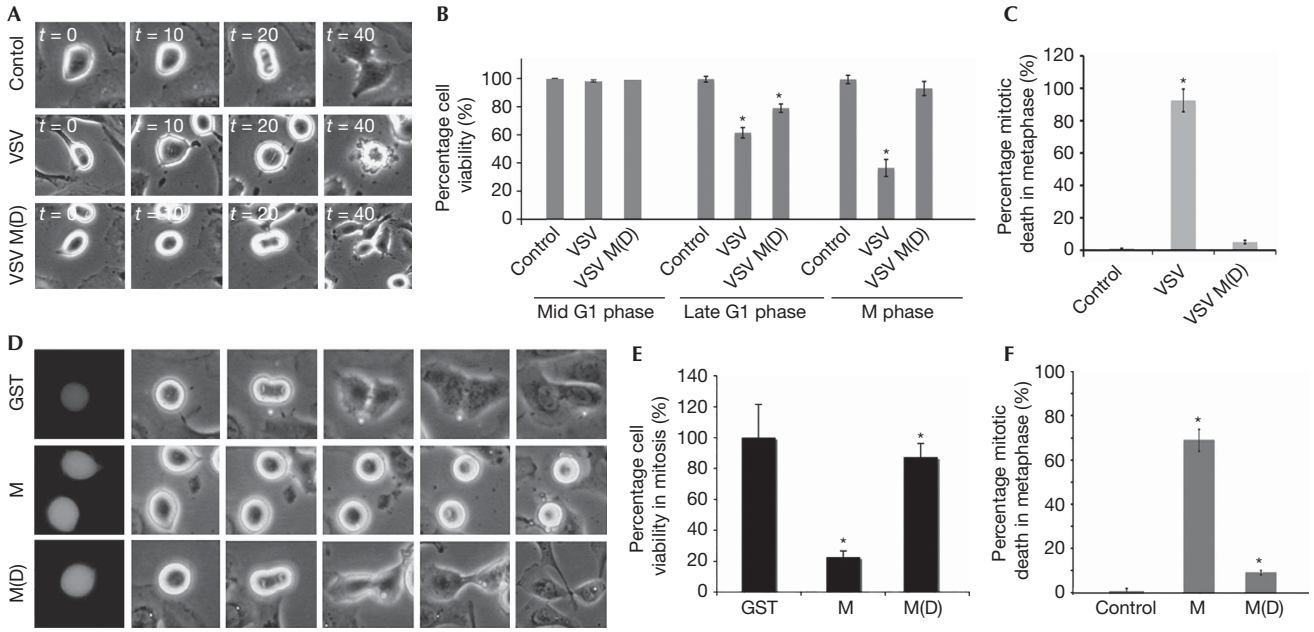

Fig 1 | Vesicular stomatitis virus hinders metaphase progression and causes mitotic cell death through M protein. (**A**) Synchronized NRK cells were mock infected or infected for 4 h with VSV or VSV M(D) at MOI 10. Infection was carried out in late G2 phase, before mitotic entry. Cells were then followed by high-resolution time-lapse microscopy until the end of mitosis. (t = min). (**B**) Synchronized NRK cells were mock infected or infected with VSV or VSV M(D) in early G1 for 4 or 7 h at MOI 10, and cell death in G1 or mitosis (as in **A**) was quantified ($n = 60$). (**C**) Mitotic cell death that occurred during metaphase (in **B**) was quantified. (**D**) NRK cells were microinjected after nuclear envelope breakdown with GST, GST–M or GST–M(D) proteins along with FITC-dextran, as an injection marker. Injected cells were followed by time-lapse microscopy. (**E**) Data obtained in (**D**) were analysed and the percentage of viable cells was plotted. (**F**) Data obtained in (**D**) were analysed and the percentage of cell death in metaphase was plotted. *$P < 0.001$. FITC, fluorescein isothiocyanate; GST, glutathione-*S*-transferase; M, matrix; MOI, multiplicity of infection; NRK, normal rat kidney; VSV, vesicular stomatitis virus.

Thus, normal rat kidney (NRK) cells synchronized in early G1 were infected with VSV and examined by time-lapse microscopy. Cell death was scored after 4 and 7 h, when cells were in mid G1 or at the end of G1, respectively. Another population of cells was infected just before entering mitosis and studied until the end of mitosis. In NRK cells, the duration of mitosis is approximately 45 min to 1 h. Mitotic progression was analysed by time-lapse microscopy, in the absence of any drug, and cell death was quantified. Cells infected with VSV showed either a block or delay in the metaphase–anaphase transition, which resulted in significant cell death during metaphase (Fig 1A–C). Some of the cells blocked in metaphase took an additional 3 h to die, therefore, we analysed cells both in G1 and in mitosis for 4 h and scored cell death (Fig 1A–C). Cell death of NRK cells in mitosis was more prominent (~70%) than in G1 (0% at 4 h and ~40% at 7 h), despite the fact that mitosis is a much shorter phase than G1. From the roughly 70% of NRK cells that died in mitosis, about 90% died in metaphase.

We then engineered a VSV that expressed a mutant of M protein that binds to very low amounts of the Rae1–Nup98 complex as compared to the strong interaction observed with the wild-type M protein (Fig 2); this mutant did not inhibit bulk mRNA export (von Kobbe *et al*, 2000; Faria *et al*, 2005). Residues 52–54 were changed to alanine in the mutant M protein. The mutant virus, VSV M(D), had little or no effect on the metaphase–anaphase transition (Fig 1A–C). In HeLa cells infected with VSV, approximately 40% of cells died in metaphase, and an additional roughly 50% of the cells were delayed during the metaphase–anaphase transition and late mitosis. The latter eventually died in late mitosis or as they entered G1 phase (supplementary Fig S1 online). These effects were attenuated when cells were infected with VSV M(D) (supplementary Fig S1 online). Our findings showed that VSV-mediated mitotic cell death contributes significantly to the cytotoxicity of VSV in proliferating cells.

M protein blocks mRNA export in interphase (Her *et al*, 1997; von Kobbe *et al*, 2000; Enninga *et al*, 2002; Faria *et al*, 2005). To further confirm that the mitotic effect observed in VSV-infected cells was not due to potential carry-over effects of M protein from interphase, we microinjected purified recombinant glutathione-*S*-transferase–M (GST–M) protein directly into mitotic cells after nuclear envelope breakdown and examined mitotic progression by time-lapse microscopy (Fig 1D). As controls, we used GST–M(D) mutant protein or GST (Fig 1D). Approximately 80% of the cells injected with VSV M protein died during mitosis, and the majority of these cells (~70%) were blocked and died during metaphase (Fig 1D–F). Conversely, no marked defects were observed in metaphase transition or cell viability in cells injected with GST control; however, a small effect was observed with the M(D) mutant protein (Fig 1E,F). Altogether, these results point to a specific effect of VSV M protein in blocking or inhibiting metaphase progression, thus causing cell death.

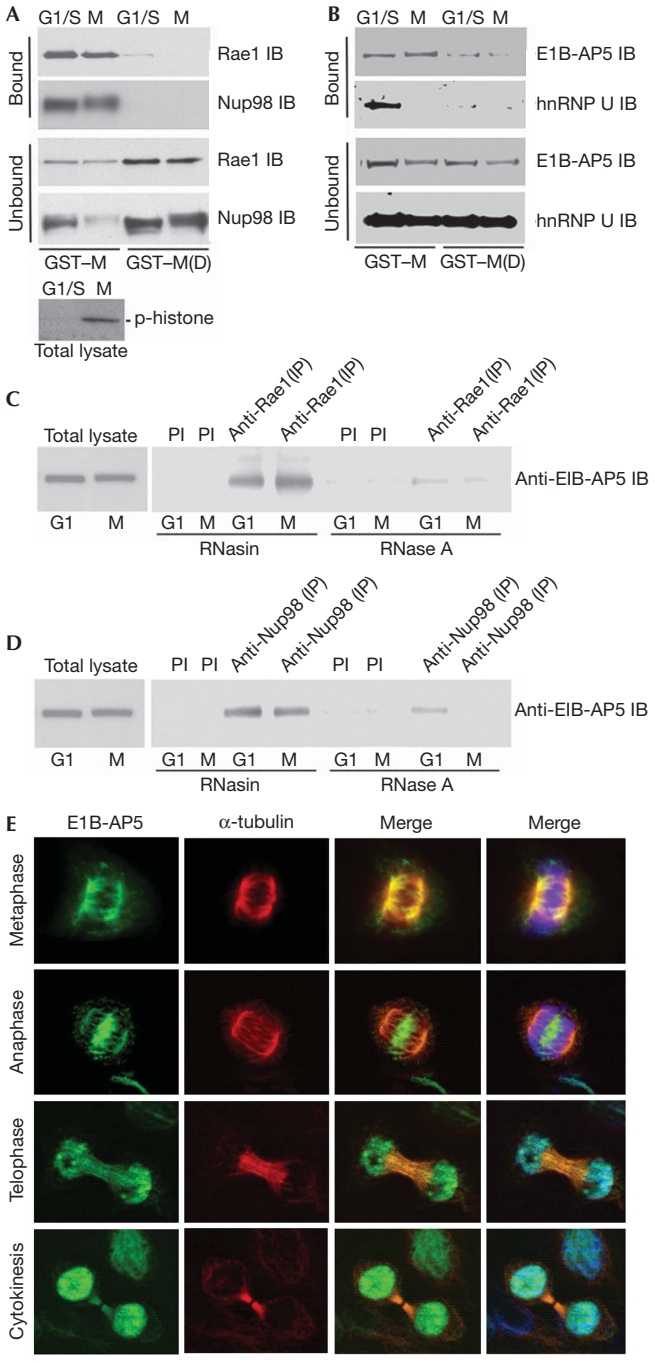

Fig 2 | VSV M protein interacts with the Rae1–Nup98 complex during both interphase and mitosis. (**A**,**B**) HeLa cell lysates synchronized at the G1/S boundary and at mitosis were incubated with immobilized recombinant GST–M or GST–M(D) proteins. Bound fractions were analysed by SDS–PAGE, and immunoblot (IB) analysis was carried out with Rae1, Nup98, EIB-AP5 or hnRNP U antibodies. Total lysates were subjected to IB analysis with phospho-histone H3 (Ser 28) antibody. (**C**,**D**) Mitotic and G1/S lysates were subjected to immunoprecipitation (IP) with Rae1 or Nup98 antibodies in the presence of RNasin or RNase A. Samples were subjected to SDS–PAGE and immunoblot analysis was carried out by using E1B-AP5 antibodies. (**E**) Cells in mitosis were subjected to immunofluorescence with E1B-AP5 and α-tubulin antibodies followed by Apotome microscopy. GST, glutathione-*S*-transferase; hnRNP, heterogeneous nuclear ribonucleoprotein; M, matrix; SDS–PAGE, sodium dodecyl sulphate polyacrylamide gel electrophoresis; VSV, vesicular stomatitis virus.

VSV M interacts with Rae1–Nup98–RNP during mitosis

VSV M protein binds to the Rae1–Nup98 complex during interphase (Faria *et al*, 2005) and VSV M(D), which expresses an M protein unable to interact strongly with Rae1, does not efficiently inhibit the metaphase–anaphase transition (Fig 1). These results suggest that abrogation of Rae1 function by M protein during mitosis significantly hampers metaphase progression. To test whether M protein binds to the Rae1–Nup98 complex during mitosis, we carried out *in vitro* binding assays using purified GST–M protein, GST–M(D) protein or GST alone, and cell lysates obtained from HeLa cells synchronized at G1/S phase or in mitosis. As shown in Fig 2A, wild-type M protein interacted with both Rae1 and Nup98 during interphase as well as during mitosis, whereas GST–M(D) protein or GST showed little or no interaction, respectively. The synchrony of the mitotic samples was determined by the presence of phospho-histone (Fig 2A). Identical results were obtained with extracts from NRK cells (data not shown).

We then investigated whether heterogeneous nuclear ribonucleoproteins (hnRNPs) would interact with the Rae1–Nup98–M complex, as RNA was shown to be important for the Rae1 function in spindle assembly (Blower *et al*, 2005). In addition, it has been demonstrated that specific classes of mRNA are associated with mitotic spindles (Blower *et al*, 2007). Therefore, we tested various hnRNPs for their ability to interact with the Rae1–Nup98–M complex. We found that the hnRNP U-like protein E1B-AP5 strongly bound to the Rae1–Nup98–M complex during interphase and mitosis, whereas hnRNP U only interacted with this complex during interphase (Fig 2B). Other hnRNPs, such as hnRNP K/J and hnRNP A1, did not show significant interaction with the complex (data not shown). These results indicate that M protein binds to the Rae1–Nup98 complex, which is not identical throughout the cell cycle, and differentially interacts with hnRNPs during interphase and mitosis.

We next investigated whether EIB-AP5 interacted with the Rae1–Nup98 complex independently of M protein and whether this association was RNA dependent. Immunoprecipitation assays were carried out using Rae1 or Nup98 antibodies and with cell lysates treated with RNase or RNase inhibitor. E1B-AP5 specifically bound to the Rae1–Nup98 complex independently of M protein, and this interaction was found to be RNA dependent, as it was greatly diminished in the presence of RNase (Fig 2C,D). We then investigated the localization of E1B-AP5 during mitosis and found that a significant pool of E1B-AP5 is associated with the spindles and another fraction is present in the mitotic cytosol during metaphase. The localization of E1B-AP5 at the spindles is compatible with a role for RNP particles in spindle assembly (Blower *et al*, 2005, 2007). EIB-AP5 is then localized at the spindle mid-zone during anaphase and inside the nucleus during cytokinesis (Fig 2E).

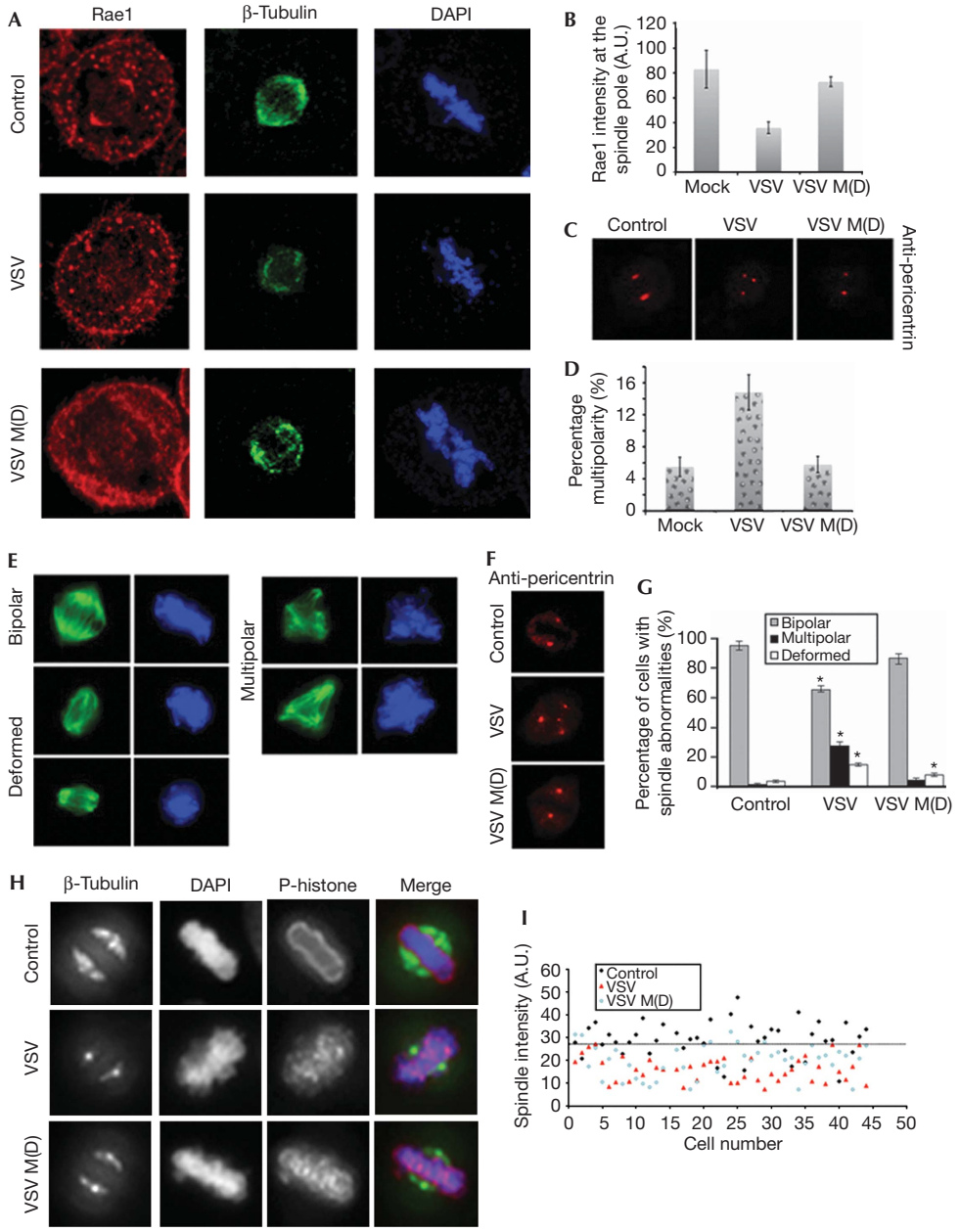

Fig 3 | VSV displaces Rae1 from the spindle pole, resulting in many spindle abnormalities. (**A**,**B**) HeLa cells were mock infected or infected with VSV or VSV M(D) as in Fig 1A or supplementary Fig S1 online, before entering mitosis. Cells were subjected to immunofluorescence with FITC-conjugated β-tubulin and Rae1 antibodies, and examined by confocal microscopy and by using a Metasystems Zeiss microscope. (**B**) Average fluorescence intensity of Rae1 staining at the spindle pole (shown in **A**) was measured by using Adobe Photoshop CS3 ($n = 30$), $^*P < 0.001$. (**C**,**D**) HeLa cells were mock infected or infected with VSV M(D) as in (**A**) and subjected to immunofluorescence using pericentrin antibody. The number of cells that showed multipolar spindles is quantified in (**D**; $n = 100$), $P < 0.001$. (**E**,**F**) NRK cells were infected with VSV as in (**A**) and subjected to immunofluorescence with FITC-conjugated β-tubulin or pericentrin antibodies. DAPI staining was used for the DNA. (**G**) Different types of spindle abnormality were classified, and the percentage of each phenotype is shown for mock infected, VSV-infected or VSV M(D)-infected cells ($n = 100$ for each condition), $^*P < 0.01$. (**H**) HeLa cells mock infected or infected with VSV or VSV M(D), as in (**A**), were placed on ice for 10 min. Cells were immunostained with FITC-β-tubulin antibody and analysed by using a Metasystems Zeiss microscope**.** The panels show representative spindle staining for each condition. (**I**) Fluorescence intensity at the spindles of cells in metaphase (as in **H**) was measured by using Adobe Photoshop (San Jose, CA, USA) CS3 ($n = 45$). The line represents the median intensity of the mock-infected cells. The difference in intensity of control, VSV and VSV (MD) cells was significant. $^*P < 0.0001$ between control and VSV-infected, or control and VSV M(D)-infected cells. DAPI, 4′,6-diamidino-2-phenylindole; FITC, fluorescein isothiocyanate; GST, glutathione-*S*-transferase; M, matrix; NRK, normal rat kidney; VSV, vesicular stomatitis virus.

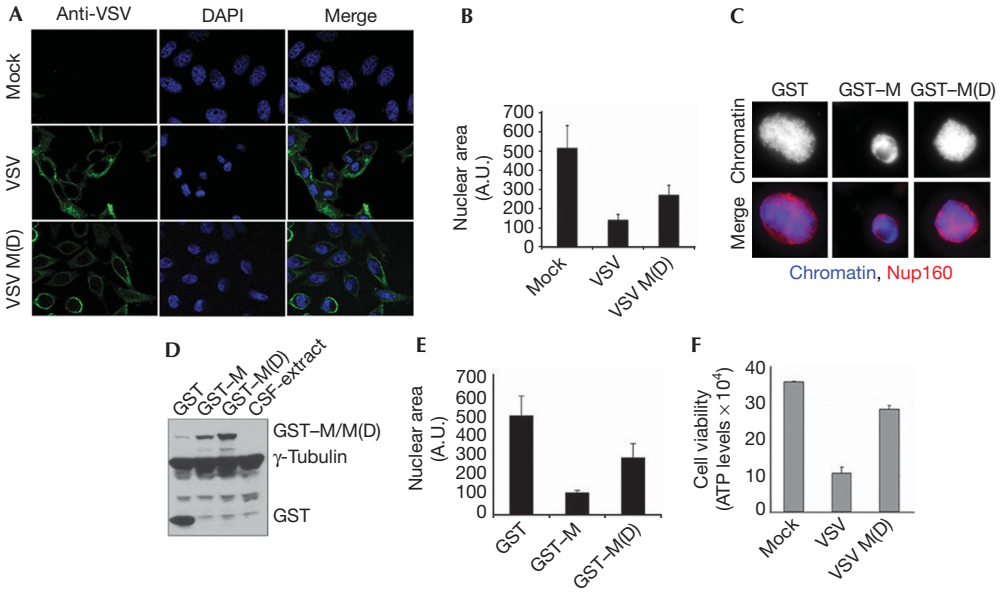

Fig 4 | VSV M protein impairs nuclei formation and chromatin decondensation. (**A**) HeLa cells were synchronized with double thymidine block at the G1/S boundary and then released into fresh medium. At 6 h post-release, cells in G2 phase were mock infected or infected with VSV or VSV M(D) at MOI 1. Cells that progressed through mitosis and entered G1 were stained with VSV antibodies, which detect cytoplasmic VSV proteins, and DAPI. (**B**) Nuclear area, for each condition shown in (**A**), was quantified using the ImageJ program (National Institutes of Health, Bethesda, MD, USA). (**C**) Interphase nuclei were formed on sperm chromatin in the presence of GST, GST–M or GST–M(D) proteins. Their growth was monitored by microscopy and the presence of the nuclear envelope was confirmed using Nup160 antibodies. (**D**) Representative samples were taken at the end of the experiments, as in (**C**), and analysed by using SDS–PAGE. Integrity of the GST, GST–M and GST–M(D) proteins was assessed by immunoblot using GST and γ-tubulin antibodies. γ-Tubulin was used as a loading control. (**E**) Nuclear area, for each condition shown in (**C**), was quantified by using the ImageJ program. (**F**) Cell viability was assessed in parallel experiments to those in (**A**), 10 h post-infection, by using the Cell Titre-Glo Luminescent cell viability assay kit (Promega, Madison, WI, USA). CSF, cytostatic factor; DAPI, 4′,6-diamidino-2-phenylindole; GST, glutathione-*S*-transferase; M, matrix; MOI, multiplicity of infection; SDS–PAGE, sodium dodecyl sulphate polyacrylamide gel electrophoresis; VSV, vesicular stomatitis virus.

VSV causes spindle abnormalities

As VSV M protein binds to the Rae1–Nup98–RNP complex during mitosis, we asked whether VSV infection would alter Rae1 localization during mitosis. HeLa cells were immunostained with Rae1 antibodies, fluorescein isothiocyanate-conjugated β-tubulin antibody or with pericentrin antibody (Fig 3A–D). As shown in Fig 3A,B, Rae1 was significantly displaced from the spindle poles. As in cells depleted of Rae1 by small interfering RNA (Blower *et al*, 2005; Wong *et al*, 2006), the M protein affected the mitotic localization of Rae1, resulting in multiple spindle abnormalities such as deformation of spindle shape, weak spindles (low microtubule density) or multipolar spindles (Fig 3). This has been shown in both NRK and HeLa cells. The formation of weak spindles was further demonstrated and quantified by examining the cold stability of kinetochore microtubules in VSV-infected cells, which showed that kinetochore microtubule stability was greatly diminished (Fig 3H,I). These results further explained the metaphase block or delay observed in VSV-infected cells due to a prolonged activation of the spindle checkpoint, which ultimately resulted in cell death. E1B-AP5 staining at the spindles was also decreased on VSV infection (supplementary Fig S2 online). VSV M(D) induced some spindle abnormality but to a much lesser extent than the wild-type virus, further corroborating a role for M protein and Rae1 in the induction of spindle damage. The slight effect of VSV M(D) on spindles could be due to the small but detectable interaction of M(D) with the Rae1–Nup98 complex (Fig 2) or due to the effects of M protein, independent of Rae1–Nup98, or other viral proteins.

VSV M protein inhibits nuclear formation

Although a substantial portion of the VSV-infected cells died during metaphase (Fig 1), a significant number of cells eventually progressed into late mitosis after a prolonged period in mitosis. We analysed these cells to determine whether VSV also has deleterious effects in telophase, cytokinesis or entry into G1 phase. Thus, cells infected with VSV or VSV M(D) in late G2 phase were followed through G1 (Fig 4A,B). Cells in G1 phase, which passed through mitosis infected with VSV, showed a reduced nuclear size compared with mock-infected cells (Fig 4A,B). Cells infected with VSV M(D) had an intermediate nuclear size between mock-infected and VSV-infected cells, indicating a role for M protein and a partial role for the Rae1–Nup98 complex in disrupting nuclear formation and chromatin decondensation (Fig 4A,B). This impaired nuclear growth is consistent with the depletion of Nup98 in reconstituted nuclei, as previously reported (Powers *et al*, 1995). At the same time, VSV infection resulted in a delay in cytokinesis in both VSV- and VSV M(D)-infected cells. These findings indicate that the cytokinesis defect might either not involve Rae1–Nup98 functions or the small amount of the Rae1–Nup98 complex that can bind to M(D) is enough to induce the

effect. Another possibility is that the cytokinesis defect involves M protein, independently of the Rae1–Nup98 complex, and/or other viral proteins (supplementary Fig S3 online). This is an interesting topic for future investigation.

To analyse the capacity of VSV M protein to disrupt nuclear assembly under conditions that were uncoupled from mitotic exit and cytokinesis, we carried out assays using the *Xenopus* nuclear reconstitution system and purified GST–M protein, GST–M(D) or GST as a control (Fig 4C–E). The results showed that M protein markedly inhibited nuclear reassembly and also hindered chromatin decondensation, resulting in considerably smaller nuclei (Fig 4C–E). These small nuclei have intact nuclear envelopes, as shown by dextran exclusion assays (supplementary Fig S4 online). Although these nuclei support nuclear import through the Kapα/β1 pathway, import competence is possibly diminished (supplementary Fig S4 online). Accurate quantification of nuclear import is not reliable in this case because of the size difference between the control and M-protein-treated nuclei, which might be at different stages of maturation. Nuclei incubated with mutant M(D) protein showed a decrease in size as compared with control, but to a much lesser extent than M-protein-treated nuclei, implying that the M protein effect was partly mediated by the Rae1–Nup98 complex (Fig 4C–E). Thus, VSV infection has profound effects on mitotic spindle assembly and post-mitotic nuclear assembly. Both of these pathways contribute to the death of infected cells, in a manner that is attenuated in VSV M(D) mutant virus for the reasons discussed above (Fig 4F).

The results shown here revealed mechanisms used by VSV to kill cells, a process that is important for its oncolytic activity. As an oncolytic agent, VSV preferentially kills tumour cells, which undergo mitosis, as compared with wild-type cells that, in animals, are normally in G0 phase (Stojdl *et al*, 2003; Barber, 2004, 2005). Thus, mitotic death might represent an acute and efficient way to kill cells at a phase in the cell cycle that the innate immune response cannot be triggered. Interestingly, it has been shown that VSV oncolysis in T lymphocytes requires cell-cycle entry (Oliere *et al*, 2008). It is possible that increasing mitotic events, by inducing T-cell proliferation, could make proliferating T cells more susceptible to VSV-mediated cell death during mitosis. Thus, VSV might be used in cancer therapy, alone or in combination with other antimitotic/anticancer drugs such as paclitaxel (taxol), to efficiently target mitotic tumour cell death. In addition, VSV might be an interesting tool for the discovery of new mitotic factors and regulators.

METHODS

Cell synchronization and infections. To assess the effects of VSV in mitosis, NRK cells were synchronized in S phase by using 2 mM thymidine for 16 h, released from the block into fresh medium for 8 h, and incubated again with 2 mM thymidine for 16 h. Cells were released into fresh medium and infected in late G2 phase before entering mitosis. For G1 synchronization, NRK cells were subjected to double thymidine block as above and released into fresh medium for 9.5 h, when cells were infected in early G1. HeLa cell synchronization, at the G1/S border, was carried out with 2 mM thymidine for 15 h, followed by a 9-h release in fresh medium, and a second incubation with 2 mM thymidine for 15 h. Cells were then released into fresh medium for 6 h to obtain synchronized samples in G2, and infections, using VSV, were carried out in late G2, 2 h before mitosis. Cells were infected at the indicated multiplicity of infections. Recombinant VSV M(D) was generated by mutating residues 52–54 of wild-type M to alanines. The virus was assembled as previously reported by Obuchi *et al* (2003).

Cell death assays. Assays were carried out by using the Cell Titre-Glo Luminescent cell viability assay kit (Promega, Madison, WI, USA).

***Xenopus* nuclear reassembly assay.** M-phase-arrested (cytostatic factor) *Xenopus* egg extract was prepared as described by Orjalo *et al* (2006), and driven into interphase by the addition of 0.6 mM $CaCl_2$. Sperm nuclei (1,500/μl) were added to the interphase extracts, along with GST, GST–M and GST–M(D) proteins. Nuclei were allowed to form during incubations at 23 °C. After 60 min, aliquots were pelleted onto cover slips and processed, for immunofluorescence, with Nup160 antibodies for nuclear envelope staining and Hoechst 33342 to visualize DNA. At the same time, equal volumes of each reaction were subjected to sodium dodecyl sulphate polyacrylamide gel electrophoresis (SDS–PAGE) and analysed by immunoblot with GST antibodies.

***In vitro* binding assays.** *In vitro* binding assays were carried out as described by Faria *et al* (2005). GST–M or GST–M(D) protein was incubated with whole-cell lysates of cells synchronized during G1/S, as described above, or during mitosis. Mitotic cells were obtained by enrichment at the G1/S border with thymidine, for 18 h, and then release of the cells into fresh medium. Nocodazole, only used for the results shown in Fig 3, was added at 7 h post-release, and cells in metaphase were shaken off and collected 5 h later, as described (Chakraborty *et al*, 2008).

Antibodies. The following antibodies were used: Rae1 for immunostaining (M.D. Blower; Blower *et al*, 2005); Rae1 and Nup98 for immunoblot (Faria *et al*, 2005); phospho-histone H3 and Ser 10 (Upstate, USA); β-tubulin–fluorescein isothiocyanate (Sigma, USA); hnRNPA1 (M. Matunis); E1B-AP5 (Proteintech Group, USA); pericentrin (Abcam, USA); monoclonal GST (Santa Cruz Biotechnology, USA); polyclonal γ-tubulin (Sigma); and polyclonal VSV (Balachandran & Barber, 2004).

Immunofluorescence, microinjection and time-lapse microscopy. Immunofluorescence was carried out as reported by Chakraborty *et al* (2008). Samples were analysed both by using the Metasystems (Boston, MA, USA) Zeiss Axioplan 2e with a Zeiss Axiocam HRm digital camera and a Leica (Bannockburn, IL, USA) TCS SP5 confocal microscope. Immunofluorescence using Rae1 antibody was carried out as described by Blower *et al* (2005). Microinjection was carried out as described by Wang *et al* (2008).

Immunoprecipitation assays. Assays were carried out as described by Chakraborty *et al* (2008). For RNase A or RNAsin pre-treatments, cell lysates were pre-incubated with RNAsin (1,000 units/ml) or RNase A (50 μg/ml; Ambion, Austin, TX, USA) for 15 min at 37 °C, followed by incubation on ice for 20 min.

Supplementary information is available at *EMBO reports* online (http://www.emboreports.org).

ACKNOWLEDGEMENTS

We thank M. Blower for Rae1 antibodies and K. Phelps for imaging studies carried out at University of Texas Southwestern Imaging Facility. This study was supported by National Institutes of Health R01 GM07159 and Texas HEB (Higher Education Board) 010019-0022-2006 to BMAF.

CONFLICT OF INTEREST

The authors declare that they have no conflict of interest.

REFERENCES

Balachandran S, Barber GN (2004) Defective translational control facilitates vesicular stomatitis virus oncolysis. *Cancer Cell* **5:** 51–65

Barber GN (2004) Vesicular stomatitis virus as an oncolytic vector. *Viral Immunol* **17:** 516–527

Barber GN (2005) VSV-tumor selective replication and protein translation. *Oncogene* **24:** 7710–7719

Blower MD, Nachury M, Heald R, Weis K (2005) A Rae1-containing ribonucleoprotein complex is required for mitotic spindle assembly. *Cell* **121:** 223–234

Blower MD, Feric E, Weis K, Heald R (2007) Genome-wide analysis demonstrates conserved localization of messenger RNAs to mitotic microtubules. *J Cell Biol* **179:** 1365–1373

Chakraborty P *et al* (2008) Nucleoporin levels regulate cell cycle progression and phase-specific gene expression. *Dev Cell* **15:** 657–667

Enninga J, Levy DE, Blobel G, Fontoura BM (2002) Role of nucleoporin induction in releasing an mRNA nuclear export block. *Science* **295:** 1523–1525

Faria PA, Chakraborty P, Levay A, Barber GN, Ezelle HJ, Enninga J, Arana C, van Deursen J, Fontoura BM (2005) VSV disrupts the Rae1/mrnp41 mRNA nuclear export pathway. *Mol Cell* **17:** 93–102

Her L-S, Lund E, Dahlberg JE (1997) Inhibition of Ran guanosine triphosphatase-dependent nuclear transport by the matrix protein of vesicular stomatitis virus. *Science* **276:** 1845–1848

Jeganathan KB, Malureanu L, van Deursen JM (2005) The Rae1–Nup98 complex prevents aneuploidy by inhibiting securin degradation. *Nature* **438:** 1036–1039

Obuchi M, Fernandez M, Barber GN (2003) Development of recombinant vesicular stomatitis viruses that exploit defects in host defense to augment specific oncolytic activity. *J Virol* **77:** 8843–8856

Oliere S, Arguello M, Mesplede T, Tumilasci V, Nakhaei P, Stojdl D, Sonenberg N, Bell J, Hiscott J (2008) Vesicular stomatitis virus oncolysis of T lymphocytes requires cell cycle entry and translation initiation. *J Virol* **82:** 5735–5749

Orjalo AV, Arnaoutov A, Shen Z, Boyarchuk Y, Zeitlin SG, Fontoura B, Briggs S, Dasso M, Forbes DJ (2006) The Nup107–160 nucleoporin complex is required for correct bipolar spindle assembly. *Mol Biol Cell* **17:** 3806–3818

Powers MA, Macaulay C, Masiarz FR, Forbes DJ (1995) Reconstituted nuclei depleted of a vertebrate GLFG nuclear pore protein, p97, import but are defective in nuclear growth and replication. *J Cell Biol* **128:** 721–736

Stojdl DF *et al* (2003) VSV strains with defects in their ability to shutdown innate immunity are potent systemic anti-cancer agents. *Cancer Cell* **4:** 263–275

von Kobbe C, van Deursen JM, Rodrigues JP, Sitterlin D, Bachi A, Wu X, Wilm M, Carmo-Fonseca M, Izaurralde E (2000) Vesicular stomatitis virus matrix protein inhibits host cell gene expression by targeting the nucleoporin Nup98. *Mol Cell* **6:** 1243–1252

Wang Y, Wei JH, Bisel B, Tang D, Seemann J (2008) Golgi cisternal unstacking stimulates COPI vesicle budding and protein transport. *PLoS ONE* **3:** e1647

Wong RW, Blobel G, Coutavas E (2006) Rae1 interaction with NUMA is required for bipolar spindle formation. *Proc Natl Acad Sci USA* **103:** 19783–19787